Structural aspects of PbO–P$_2$O$_5$ glasses containing ThO$_2$

C.G.S. Pillai *, V. Sudarsan, M. Roy, A.K. Dua

Novel Materials and Structural Chemistry Division, Bhabha Atomic Research Centre, Mumbai 400085, India

Abstract

PbO–P$_2$O$_5$ glasses in which part of PbO/P$_2$O$_5$ was replaced by ThO$_2$ have been prepared by the conventional melt quench method and their structural aspects have been studied by ^{31}P MAS NMR, Raman and FTIR techniques. Binary PbO–P$_2$O$_5$ glass is characterized by mainly Q^2 and Q^1 structural units of P (Q^n represents the phosphorus structural units having 'n' number of bridging oxygen atoms). When part of the PbO has been replaced by ThO$_2$, the phosphorus structural units are not significantly affected, indicating that Th^{4+} replaces Pb^{2+} at the interstitial positions in the glass network. Unlike this when part of P$_2$O$_5$ has been replaced by ThO$_2$ extensive depolymerisation of the phosphate network resulted in the conversion of Q^2 to Q^1 structural units of P. Above 10 mol% of ThO$_2$ replacement in either case resulted in the partial devitrification of the glass.
© 2003 Elsevier B.V. All rights reserved.

1. Introduction

Phosphate based glasses are technologically important and are widely used for making solid-state electrolytes, machinable glass ceramics etc. [1–4]. Many of the phosphate-based glasses are low melting and glass formation takes place over a wide composition range. However, the chemical stability due to hygroscopic nature of many of these glasses poses a serious problem for various technological applications. The hygroscopic nature of phosphate glasses arises mainly because of the presence of phosphorus structural units with nonbridging oxygen atoms, which can react with moisture to form phosphoric acid, which is detrimental to the glass [5]. In general, the chemical stability and other physical properties of these glasses can be modified by adding a variety of oxides. For example addition of Al$_2$O$_3$, Sb$_2$O$_3$, Fe$_2$O$_3$ etc. to phosphate glasses has been found to improve the stability and modify the physico-chemical properties like thermal expansion coefficient, electrical conductivity, cut-off wavelength in the UV–visible region etc. [6–8], which have been attributed to the formation of P–O–Al, P–O–Sb, P–O–Fe etc. linkages. Thus, the knowledge regarding the structural aspects of these glasses is essential to understand the physico-chemical properties of the glasses. Solid-state magic angle spinning nuclear magnetic resonance (MAS NMR) combined with Raman and Fourier transform infrared (FTIR) techniques can give valuable information regarding different types of structural units present in the glass. For example, binary PbO–P$_2$O$_5$ and PbO–P$_2$O$_5$ glasses having additives like Sb$_2$O$_3$ and ZnO have been well studied by various authors [7,9,10] for understanding the nature of different structural units constituting the glass.

ThO$_2$ is one of the components present along with high level wastes like Cs^{137}, Sr^{90}, Ru^{160} etc. generated in nuclear reactors based on thoria fuels, which has to be immobilised for final geological disposal. With a view to explore the possibility of incorporation of ThO$_2$ in PbO–P$_2$O$_5$ glasses, as well as to improve the stability of PbO–P$_2$O$_5$ glasses, we have prepared a series of PbO–P$_2$O$_5$ glasses, with varying amounts of ThO$_2$ and investigated their structural aspects using various techniques. This paper deals with the ^{31}P MAS NMR, Raman and FTIR spectroscopic studies of these glasses to elucidate their structural aspects at microscopic level.

---

* Corresponding author. Tel.: +91-22 255 95355; fax: +91-22 255 05151.
  E-mail address: cgspil@apsara.barc.ernet.in (C.G.S. Pillai).

2. Experimental

$(PbO)_{1-x}(P_2O_5)_x$ glasses made with a starting composition of $x = 0.5$, in which either PbO or P_2O_5 has been partly replaced by ThO_2 (up to 10 mol%), were prepared by conventional melt quench method. Stoichiometric quantities of reagent grade PbO, ThO_2 and $NH_4H_2PO_4$ were ground, thoroughly mixed and preheated to 725 K for 2 h. The charge was then ground again and melted in an alumina crucible at temperatures between 1275 and 1475 K, depending on the composition. Finally, the melt was quenched in between two stainless steel plates. X-ray diffraction measurements were made on a Philips diffractometer PW1710 using the Cu Kα radiation.

The ^{31}P MAS NMR spectra of these samples were recorded using a Bruker Avance DPX 300 unit with a Larmor frequency of 121.34 MHz. The samples were packed inside 7 mm zirconia rotors and subjected to a spinning frequency of 5 kHz. Typical 90° pulses of $\simeq 4.5\,\mu s$ duration with a relaxation delay of 5 s were used for recording the spectra. ^{31}P MAS NMR experiments were also carried out with higher delay times like 45 and 60 s and the NMR patterns obtained were found to be identical with that recorded with a delay time of 5 s. Since the relaxation time is inversely related to line width, higher line widths of ^{31}P MAS NMR patterns of glassy materials indicate faster relaxation, thereby giving rise to NMR patterns with higher signal-to-noise ratios even with smaller delay times. The chemical shifts are reported with respect to 85% H_3PO_4 solution as the reference. Raman spectra were recorded ex-situ under microconfiguration in a back scattering geometry with a spectral resolution of $\simeq 2\ cm^{-1}$. The 514.5 nm ($\simeq 2.4$ eV) line of Ar^+ laser with a power of $\simeq 10$ mW, focused on to a spot of $\simeq 1\,\mu m$ in diameter using 100× microscope objective was used for excitation. The Raman shifted scattered light was analyzed using an optically aligned single stage microRaman spectrometer (Dilor_Jobin Yvon_Spex) equipped with a charge coupled device (CCD) camera for multichannel detection. Spectra were recorded at different positions on the sample for any possible spatial inhomogeneity in the sample. Finally, the Raman spectra were normalized to the incident power and time of accumulation. For infrared investigations, glass samples were ground thoroughly along with KBr. The fine powders obtained thus were finally pressed in the form of thin pellets. Infrared absorption spectra were recorded by using a Bomem MB 102 spectrophotometer, over 4000–200 cm^{-1} with a resolution of 4 cm^{-1}.

3. Results and discussion

XRD patterns of all the samples gave a broad hump over the region 20°–35° characteristic of their amorphous nature. Representative patterns are shown in Fig. 1. Incorporation of ThO_2 above 10 mol% resulted in the partial devitrification of the glass as revealed by the appearance of sharp peaks in the XRD patterns of corresponding samples. Fig. 2 shows the ^{31}P MAS NMR patterns of PbO–ThO_2–P_2O_5 glasses. For binary $(PbO)_x(P_2O_5)_{1-x}$ glass with a starting composition of $x = 0.5$, the ^{31}P MAS NMR pattern contains mainly two peaks, placed at around −24 and −10 ppm. Based on the ^{31}P MAS NMR studies of inorganic phosphate glasses and crystalline compounds, the peak around −10 ppm has been attributed to phosphorus structural units having one bridging oxygen atom (Q^1) and the peak around −24 ppm can be attributed to phosphorus structural units having two bridging oxygen atoms (Q^2) [6,11,12]. It is expected that for $(PbO)_{0.5}(P_2O_5)_{0.5}$ glass, there should not be any Q^1 structural units. However, in the present study we observed the presence of Q^1 structural units for the above composition, which has been attributed to the loss of P_2O_5 due to volatilization, during melting. Based on the composition dependence of the Q^n structural units reported for various phosphate glasses [13,14], the actual composition of the glass has been calculated and found to be $(PbO)_{0.54}(P_2O_5)_{0.46}$. Similar calculations have been carried out for all the glass compositions studied and are given in Table 1.

It has been established that in PbO containing glasses, Pb exists as Pb^{2+} and it can act both as network modifier as well as network former [9]. When it acts as a network modifier, Pb^{2+} goes and sits in the interstitial position in the glass network and neutralizes the negative charge of non-bridging oxygen attached to phos-
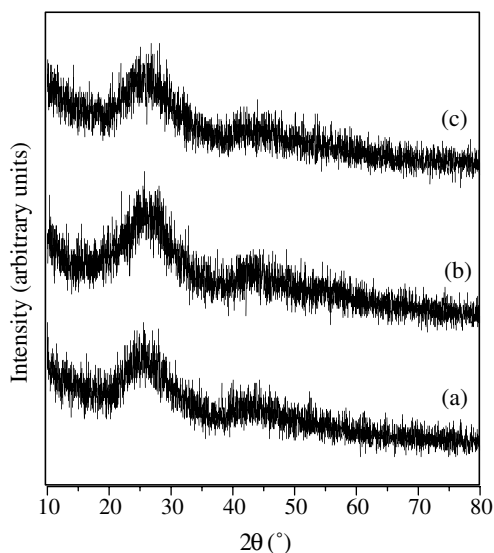

Fig. 1. XRD patterns of (a) $(PbO)_{0.54}(P_2O_5)_{0.46}$, (b) $(PbO)_{0.45}$-$(ThO_2)_{0.10}(P_2O_5)_{0.45}$ and (c) $(PbO)_{0.55}(P_2O_5)_{0.35}(ThO_2)_{0.10}$ glasses.
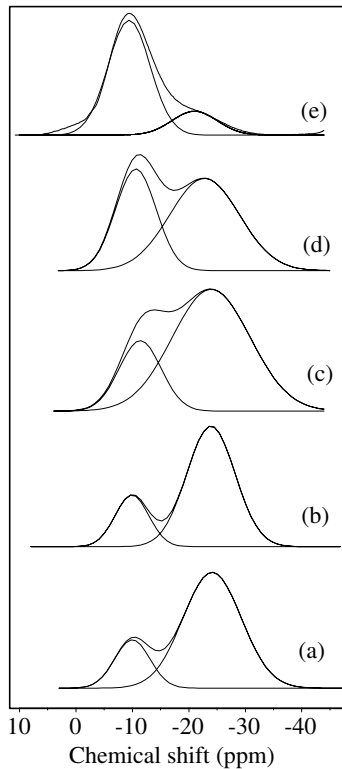
Fig. 2. ^{31}P MAS NMR spectra of (a) $(PbO)_{0.54}(P_2O_5)_{0.46}$, (b) $(PbO)_{0.50}(ThO_2)_{0.05}(P_2O_5)_{0.45}$, (c) $(PbO)_{0.45}(ThO_2)_{0.10}(P_2O_5)_{0.45}$, (d) $(PbO)_{0.53}(P_2O_5)_{0.42}(ThO_2)_{0.05}$ and (e) $(PbO)_{0.55}(P_2O_5)_{0.35}$-$(ThO_2)_{0.10}$ glasses.

Table 1
Q^1 & Q^2 fractions estimated from NMR patterns along with different glass compositions

Compositions	$[Q^2]$	$[Q^1]$
$(PbO)_{0.54}(P_2O_5)_{0.46}$	0.80	0.20
$(PbO)_{0.50}(ThO_2)_{0.05}(P_2O_5)_{0.45}$	0.77	0.23
$(PbO)_{0.45}(ThO_2)_{0.10}(P_2O_5)_{0.45}$	0.76	0.24
$(PbO)_{0.53}(P_2O_5)_{0.42}(ThO_2)_{0.05}$	0.61	0.39
$(PbO)_{0.55}(P_2O_5)_{0.35}(ThO_2)_{0.10}$	0.18	0.82

phorus and have an octahedral configuration [9], whereas when it acts as a network former, PbO_4 structural units are connected to phosphorus structural units through P–O–Pb corner sharing linkages [9,15,16]. Partial replacement of PbO by ThO_2 up to 10 mol% resulted in the broadening of ^{31}P MAS NMR peaks. Deconvolution of these patterns based on a Gaussian fit indicated that there is slight increase in the relative fraction of Q^1 structural units from 20 to 23 and 24 mol%, respectively, for 5 and 10 mol% of ThO_2 substitution. Based on the O/P ratios, the relative concentrations of Q^1 structural

units were calculated and found to be 22.7 and 23.7 mol% respectively for $(PbO)_{0.50}(ThO_2)_{0.05}(P_2O_5)_{0.45}$ and $(PbO)_{0.45}(ThO_2)_{0.10}(P_2O_5)_{0.45}$ glasses.

As part of the PbO is replaced by ThO_2, probably the Pb^{2+} which are at the interstitial positions are substituted by Th^{4+}. Hence the relative intensities of the peak −10 and −24 ppm are only slightly affected which is in accordance with the increase of the O/P ratio. The broadening of the NMR lines can be attributed to the distribution in the chemical shift brought about by the distortion in P–O–P linkages arising due to the difference in the nuclear charges of Pb^{2+} and Th^{4+} ions. Due to the higher value of the cationic field strength of Th^{4+} ($Z/r \sim 0.042$ pm^{-1}) compared to Pb^{2+} ($Z/r \sim 0.0169$ pm^{-1}), the extent of distortion of P–O–P linkages of the glass network brought about by Th^{4+} is a greater extent as compared to Pb^{2+}. When part of the P_2O_5 is replaced by ThO_2, the P–O–P network got depolymerised resulting in the systematic conversion of Q^2 to Q^1 structural units.

Fig. 3 shows the Raman spectra of PbO–P_2O_5–ThO_2 glasses. Binary $(PbO)_{0.54}(P_2O_5)_{0.46}$ glass has been found to consists of a sharp peak $\simeq 1150$ cm^{-1} along with less intense shoulder peaks $\simeq 1210$ and 1034 cm^{-1} and an asymmetric peak $\simeq 693$ cm^{-1}. Based on the Raman studies of various phosphate glasses containing PbO [9,16], the sharp peak $\simeq 1150$ cm^{-1} and the shoulder peak $\simeq 1210$ cm^{-1} have respectively been assigned to the symmetric and asymmetric stretching of PO_4 tetrahedra

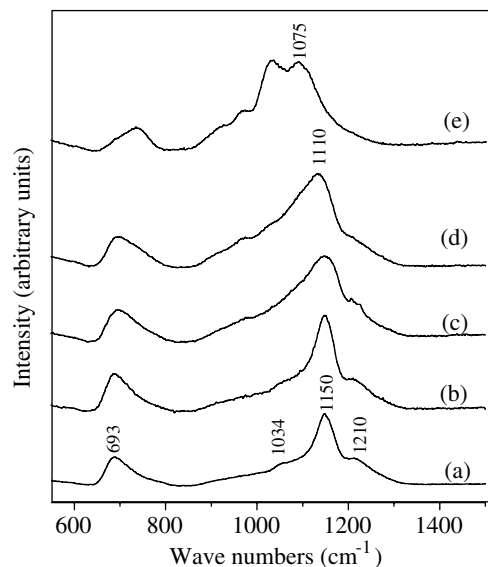Fig. 3. Raman spectra of (a) $(PbO)_{0.54}(P_2O_5)_{0.46}$, (b) $(PbO)_{0.50}(ThO_2)_{0.05}(P_2O_5)_{0.45}$, (c) $(PbO)_{0.45}(ThO_2)_{0.10}(P_2O_5)_{0.45}$, (d) $(PbO)_{0.53}(P_2O_5)_{0.42}(ThO_2)_{0.05}$ and (e) $(PbO)_{0.55}(P_2O_5)_{0.35}$-$(ThO_2)_{0.10}$ glasses.

with 2 non-bridging oxygen atoms [9]. The peak $\simeq 693$ cm^{-1} has been assigned to the asymmetric stretching of P–O–P bridging bonds. Shoulder peak $\simeq 1034$ cm^{-1} corresponds to the existence of pyrophosphate groups $[(P_2O_7)^{4-}]$ [9]. As part of the PbO is replaced by ThO$_2$, the Raman peaks got slightly broadened but the peak maxima remained more or less same. Unlike this, when part of the P$_2$O$_5$ is replaced by ThO$_2$ in addition to the line broadening, the peak $\simeq 1150$ cm^{-1} shifted systematically to lower wave numbers namely 1110 and 1075 cm^{-1}. Further the relative intensity of the peak around 1034 cm^{-1} increased considerably which has been attributed to the formation of more pyrophosphate structural units due to the higher extent of depolymerisation brought about by Th^{4+}. The broadening of the peaks can be attributed to the increase in disorder of phosphorus structural units resulted by the presence of Th^{4+} in the glass network, which is also seen in the ^{31}P MAS NMR patterns. Had ThO$_2$ acted as a network former in PbO–P$_2$O$_5$ glasses, the P–O–P network of the glass would have become stronger as $(Z/r)_{Th^{4+}} > (Z/r)_{Pb^{2+}}$, resulting in the shifting of the stretching frequencies to higher wave numbers. Once the covalent bonds get destroyed to form ionic bonds, the P–O–P linkages gets weakened resulting in the shifting of the Raman peaks to lower values. This indicates that ThO$_2$ acts as a network modifier.

Fig. 4 shows the representative FTIR patterns of PbO–P$_2$O$_5$ glasses containing different amounts of ThO$_2$. Binary $(PbO)_{0.54}(P_2O_5)_{0.46}$ glass is characterized by strong bands in the regions of 1265, 1087, 897, 716

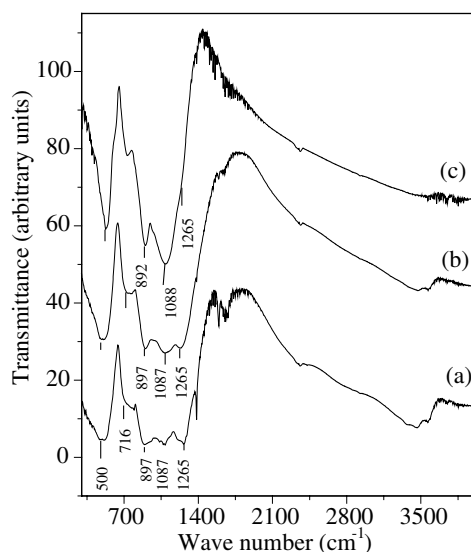and 500 cm^{-1}. Different vibrational modes of PbO and ThO$_2$ are not observed in these patterns as they absorb below 400 cm^{-1}. The peaks around 1265 and 1087 cm^{-1} have been respectively assigned to the asymmetric and symmetric stretching vibrations of P structural units having two non-bridging oxygen atoms, O–P–O, (PO$_2$) units [17–20], which is also observed in the Raman spectra. The corresponding modes for the P–O–P linkages appear at $\simeq 900$ and 700 cm^{-1}. The peak around 500 cm^{-1} has been attributed to the deformation modes of phosphate tetrahedra [20]. When part of the PbO has been replaced by ThO$_2$, the relative intensities of the peaks around 1265, 1088 and 897 cm^{-1} remain unaffected. However, the relative intensities of the 1265 cm^{-1} peak decreases and the one at 1088 cm^{-1} increases when part of the P$_2$O$_5$ has been replaced by ThO$_2$. The change in the relative intensities can be attributed to the change in the transition probabilities corresponding to the symmetric stretching of PO$_2$ linkages mentioned above brought about by the Q^2 to Q^1 conversion. At this point it is worthwhile to mention that such changes in the relative intensities were also observed in the Raman spectra. The considerable reduction of the intensity of the broad peak at $\simeq 3400$ cm^{-1} arising from moisture in the IR pattern for $(PbO)_{0.54}(P_2O_5)_{0.46-y}(ThO_2)_y$ glasses indicates the improved stability of these glasses.

Thus based on the ^{31}P MAS NMR, Raman and FTIR spectroscopic studies of these glasses, it has been established that when part of the PbO is replaced by ThO$_2$ in $(PbO)_{0.54}(P_2O_5)_{0.46}$ glass, Th^{4+} substitutes at the interstitial site. However, when P$_2$O$_5$ is replaced by ThO$_2$, depolymerisation of P–O–P linkages results in the formation of more discrete phosphorus structural units. Further based on these studies, it can be inferred that ThO$_2$ acts as network modifier.

4. Conclusions

Binary $(PbO)_{0.54}(P_2O_5)_{0.46}$ glass mainly contains Q^2 and Q^1 structural units of phosphorus. Partial replacement of PbO by ThO$_2$ up to 10 mol%, results in the substitution of Th^{4+} at the interstitial site. Unlike this when part of the P$_2$O$_5$ was replaced by ThO$_2$, the P–O network got extensively depolymerised, resulting in the systematic conversion of Q^2 to Q^1 structural units of phosphorus. Incorporation of ThO$_2$ above 10 mol% resulted in the partial devitrification of the glass.

Fig. 4. FTIR spectra of (a) $(PbO)_{0.54}(P_2O_5)_{0.46}$, (b) $(PbO)_{0.45}$-$(ThO_2)_{0.10}(P_2O_5)_{0.45}$ and (c) $(PbO)_{0.55}(P_2O_5)_{0.35}(ThO_2)_{0.10}$ samples.

References

[1] J. Zarzycki, in: R.W. Cahn, P. Haasen, E.J. Kramer (Eds.), Material Science and Technology, vol. 9, VCH, Weinheim, 1991.

[2] C.R. Bamford, Colour Generation and Control in Glasses, Elsevier, Amsterdam, 1977.

[3] C.S. Ray, X. Fang, M. Karabulut, G.K. Marasinghe, D.E. Day, J. Non-Cryst. Solids 249 (1999) 1.

[4] M. Karabulut, G.K. Marasinghe, C.S. Ray, D.E. Day, O. Ozturk, G.D. Waddill, J. Non-Cryst. Solids 249 (1999) 106.

[5] G.D. Khattak, E.E. Khawaja, L.E. Wenger, D.J. Thompson, M.A. Salim, A.B. Hallak, M.A. Daous, J. Non-Cryst. Solids 194 (1996) 1.

[6] R.K. Brow, J. Am. Ceram. Soc. 76 (1993) 913.

[7] G. Guo, Glass Technol. 39 (1998) 138.

[8] D.E. Day, Z. Wu, C.S. Ray, P. Hrma, J. Non-Cryst. Solids 241 (1998) 1.

[9] H.S. Liu, P.Y. Shih, T.S. Chin, Phys. Chem. Glasses 37 (1996) 227.

[10] V. Sudarsan, S.K. Kulshreshtha, J. Non-Cryst. Solids 286 (2001) 99.

[11] R.K. Brow, R.J. Kirkpatrick, G.L. Turner, J. Non-Cryst. Solids 116 (1990) 39.

[12] R.K. Brow, J. Non-Cryst. Solids 263&264 (2000) 1.

[13] J.R. Van Wazer, in: Phosphorus and its Compounds, vols. 1&2, Interscience, New York, 1967.

[14] R. Hussin, D. Holland, R. Dupree, J. Non-Cryst. Solids 298 (2002) 32.

[15] S. Prabhakar, K.J. Rao, C.N.R. Rao, Chem. Phys. Lett. 139 (1987) 96.

[16] G.B. Rouse, P.J. Miller, W.M. Risen, J. Non-Cryst. Solids 28 (1978) 193.

[17] R.K. Brow, D.R. Tallant, S.T. Myers, C.C. Phifer, J. Non-Cryst. Solids 191 (1995) 45.

[18] J.J. Hudgens, S.W. Martin, J. Am. Ceram. Soc. 76 (1993) 1691.

[19] K. Meyer, J. Non-Cryst. Solids 209 (1997) 227.

[20] M.A. Salim, G.D. Khattak, M.S. Hussain, J. Non-Cryst. Solids 185 (1995) 101.